Proceedings of the 26th Annual International Conference of the IEEE EMBS
San Francisco, CA, USA • September 1-5, 2004

Texture Analysis of the Endometrium During Hysteroscopy: Preliminary Results

M. S. Neophytou[1,4], C. S. Pattichis[1], M. S. Pattichis[1,3], V. Tanos[2], E. C. Kyriacou[1], S. Pavlopoulos[4], D. D. Koutsouris[4]

[1]Department of Computer Science, University of Cyprus, Nicosia, Cyprus, {mneoph, pattichi, mariosp, ekyriac} @ucy.ac.cy
[2]Evaggelistria Medical Center, Nicosia, Cyprus, tanosv@spidernet.com.cy
[3]Deptartment of Electrical and Computer Engineering, University of New Mexico, NM, USA
[4]Biomedical Engineering Laboratory, Department of Electrical and Computer Engineering, National Technical University of Athens, Greece, {spav, dkoutsou} @biomed.ntua.gr

Abstract — The objective of this study is to investigate the usefulness of texture analysis in the endometrium during hysteroscopy in endoscopic imaging of the uterine cavity. Endoscopy images from the endometrium from three subjects, at optimum illumination and focus, were frozen and digitized at 720x576 pixels using 24bits color. Regions of Interest (ROI) of normal (N=61) and abnormal (N=69) regions were manually selected by the physician. ROI images were converted into gray scale and Statistical Features (SF) and Spatial Gray Level Dependence Matrix features (SGLDM) were computed. The non-parametric Wilcoxon rank sum test at a = 0.05 was carried out for comparing the differences between normal and abnormal tissue. There was significant difference between normal and abnormal endometrium for the SF features variance, energy and entropy and for the SGLDM feature of angular second moment. There was no significant difference for the SF features mean, median, and SGLDM features of contrast, correlation and homogeneity.

Keywords—**Hysteroscopy, endometrium, endometrial, hyperplasia, texture analysis**

I. Introduction

Hysteroscopy is an investigation method for the diagnosis of endometrial abnormalities-pathologies. The eye piece of a telescope of 2,5mm in diameter, is connected to a camera and a monitor. The telescope is inserted through the natural cervical canal of the uterus and propagated to the endometrial cavity [1]. Using normal saline as a distention medium we can observe the endometrial cavity and diagnose endometrial abnormalities including endometrial cancer [2]. Sometimes, areas of endometrial cancer can be missed or unnecessary endometrial biopsies are performed.

The objective of this study is to investigate the usefulness of texture analysis of the endometrial tissue during hysteroscopy as well as to study texture variability at different image scales, in order to increase the sensitivity and the specificity of the diagnosis during hysteroscopy. Preliminary findings of this study were also published in [3].

Some relate work for colonoscopy images is reported in [4]-[5] for the detection of tumours in colonoscopic video. The detection rate of abnormal colonic regions corresponding to adenomatous polyps was very high. In our own previous work, we used experimental tissue comparing texture feature variability under different viewing conditions such as different angles and different distances from the imaged object. The results indicate that for small differences in consecutive angles, there is no significant variability in the values of the texture features. On the other hand, as expected, we found but there are significant differences when comparing texture feature values extracted from panoramic vs. close up views [6].

II. Methodology

A. Recording of Images

In order to capture the images, the CIRCON IP4.1 endoscopic camera was used. The analog output signal of the camera (PAL 475 horizontal lines) was digitized at 720x576 pixels using 24bit color (tiff format), using the Matrox Meteor II frame grabber. Regions of interest (ROIs) (abnormal and adjacent normal regions) were selected by an expert in three subjects as illustrated in Fig. 1. A total of 61 and 69 normal and abnormal endometrium ROIs were selected. Histopathology results for the three cases investigated revealed endometrium hyperplasia with cell atypia which is a precancerous condition.

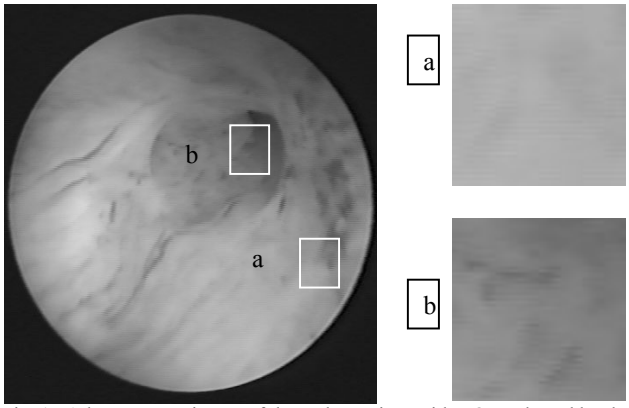

Fig. 1. A laparoscopy image of the endometrium with ROIs selected by the physician: (a) normal ROI, and (b) abnormal ROI.

B. Feature Extraction

The ROI color images were transformed into grayscale images, and the following texture features were computed:

Statistical Features (SF): SF features describe the gray level histogram distribution without considering spatial independence. The following texture features were computed: 1) Mean, 2) Variance, 3) Median, 4) Energy, and 5) Entropy.

Spatial Gray Level Dependence Matrices (SGLDM): The spatial gray level dependence matrices as proposed by Haralick et al. [7] are based on the estimation of the second-order joint conditional probability density functions that two pixels (k, l) and (m, n) with distance d in direction specified by the angle θ, have intensities of gray level i and gray level j. Based on the estimated probability density functions, the following four texture measures out of the 13 proposed by Haralick et al. [7] were computed: 1) Angular second moment (ASM), 2) Contrast, 3) Correlation, and 4) Homogeneity. For a chosen distance d (in this work $d=1$ was used), and for angles $\theta = 0^o, 45^o, 90^o$ and 135^o we computed four values for each of the above texture measures. The above features were calculated for displacements $\delta=(0,1)$, $(1,1)$, $(1,0)$, $(1,-1)$, where $\delta\equiv(\Delta x,\Delta y)$, and their range of values were computed.

C. Multiscale analysis

The goal of multiscale image analysis is to reveal image characteristics at different image resolutions [8]. For example, small objects affect texture features at low resolution levels (with little or no downsampling involved), while larger objects affect texture features at higher resolution levels. Thus, if there is a particular range of scales, where we have objects of diagnostic interest, it is preferable to use this range for feature extraction in computer aided diagnostic systems. Within a single image scale, there is a number of different frequency bands that can be used for texture feature analysis.

In this study, we only used the low-frequency band, where most of the image energy is nearly-always concentrated. This was implemented by first applying a low-pass filter, followed by downsampling by a factor of two to ten in each direction as illustrated in Fig. 2.

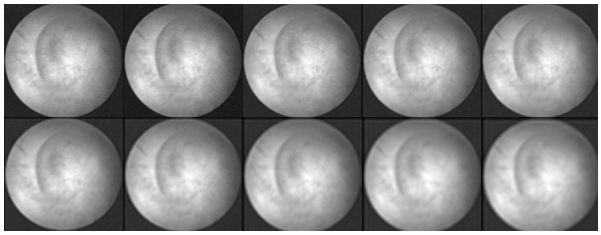

Fig. 2. Multiscale analysis of an endometrium gray scale image. Upper row: original image and images with downsampling rate 2x2 up to 5x5. Lower row: images with downsampling rate 6x6 up to 10x10.

We note that significant differences exist between the downsampled images of Fig. 2. Yet, it is not easy to observe these differences without a very careful examination. Texture features are computed for each downsampled image.

III. RESULTS

Table I summarizes the median, lower quartile (Q_1), upper quartile (Q_3), and the spread (semi inter quartile range) for the SF and SGLDM features for the normal and abnormal ROIs investigated. Also, the non-parametric Wilcoxon rank sum test was carried out to compare if there is a significant difference between normal and abnormal tissue. It is shown in Table I that there is significant difference between normal and abnormal endometrium ROIs

TABLE I
SF AND SGLDM TEXTURE FEATURES FOR THE ENDOMETRIUM (THREE SUBJECTS) {Q_1, Q_3, AND SIQR REPRESENT THE LOWER QUARTILE (25% PERCENTILE), UPPER QUARTILE (75% PERCENTILE) AND THE SEMI-INTER QUARTILE RANGE, RESPECTIVELY}

	Normal Endometrium (n=61)				Abnormal Endometrium (n=69)				
Texture	Q_1	Median	Q_3	SIQR	Q_1	Median	Q_3	SIQR	H[1]
Features	SF								
Mean	126,688	136,802	155,089	14,20093	110,563	139,661	169,185	29,31104	0
Median	127,583	138,165	155,455	13,93565	109,460	139,398	170,263	30,40107	0
Variance	28,450	49,158	100,884	36,217	60,435	91,787	149,622	44,594	1
Energy	0,031	0,041	0,054	0,012	0,025	0,032	0,040	0,007	1
Entropy	3,014	3,350	3,604	0,295	3,372	3,586	3,801	0,214	1
	SGLDM								
$ASM^2{}_{x100}$	0,36175	0,5798	0,83568	0,236965	0,34005	0,4522	0,58172	0,120835	1
Contrast	3,373	4,178	5,202	0,915	3,650	4,906	7,621	1,986	0
Correlation	0,874	0,941	0,971	0,049	0,090	0,961	0,978	0,444	0
Homogeneity	0,362	0,443	0,467	0,052	0,272	0,413	0,471	0,100	0

[1]H IS THE RESULT OF WILCOXON RANK SUM TEST BETWEEN NORMAL AND ABNORMAL TISSUE WITH '1' INDICATING SIGNIFICANT DIFFERENCE, AND '0' NO SIGNIFICANT DIFFERENCE AT A=0.05
[2]ASM=ANGULAR SECOND MOMENT

for the SF features variance, energy and entropy, and for the SGLDM feature angular second moment (see also Fig. 3 for a boxplot of the angular second moment). However, there is no significant difference between normal and abnormal endometrium for the rest of the features investigated, i.e. SF mean, median, and the SGLDM features contrast, correlation, and homogeneity (see also Fig. 4 for a boxplot of homogeneity). It is clearly shown in Table I that the SF feature variance and entropy, significantly increase between normal and abnormal endometrium, whereas the SF energy and SGLDM angular second moment significantly decrease between normal and abnormal endometrium. The SF features mean and median and the SGLDM correlation do not change between normal and abnormal whereas the SGLDM features contrast and homogeneity increase and decrease respectively between normal and abnormal endometrium.

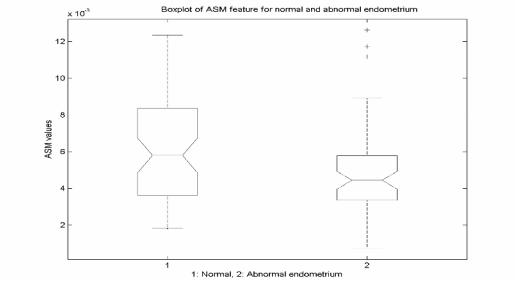

Fig. 3. Boxplot of ASM for (1) normal and (2) abnormal endometrium. The notched box shows the median, lower and upper quartiles and confidence interval around the median for each feature. The dotted line connects the nearest observations within 1.5 of the inter-quartile range (IQR) of the lower and upper quartiles. Crosses (+) indicate possible outliers with values beyond the ends of the 1.5 x IQR.

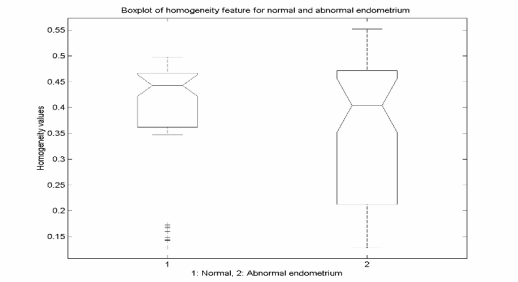

Fig. 4. Boxplot of homogeneity for (1) normal and (2) abnormal endometrium. The notched box shows the median, lower and upper quartiles and confidence interval around the median for each feature. The dotted line connects the nearest observations within 1.5 of the inter-quartile range (IQR) of the lower and upper quartiles. Crosses (+) indicate possible outliers with values beyond the ends of the 1.5 x IQR.

Figures 5 to 8 illustrate the multiscale analysis carried out for one subject for 11 normal and 11 abnormal ROIs for the features SF mean and variance, and the SGLDM angular second moment, and homogeneity respectively. It is clearly shown in Fig 5 and 6 for both normal and abnormal endometrium that the SF mean does not show significant variation with different scales, whereas the SF variance increases with scale. As illustrated in Fig. 7, the SGLDM feature angular second moment drops significantly from the 1x1 scale to the 2x2 scale, and then levels off for the rest of the scales. However, more variations are observed for the normal tissue when compared to the abnormal tissue. In Fig. 8, we see that SGLDM homogeneity varies similarly to SGLDM angular second moment but it decreases slightly with scale.

IV. Concluding Remarks

Although the results of this study are preliminary, it seems that some texture features can be used to differentiate between normal and abnormal endometrium in laparoscopy imaging. More images have to be analyzed to further support this.

Acknowledgment

This study is funded through the Research Promotion Foundation, Cyprus, PENEK 2002, Program for the Financial Support of New Researchers, through the project entitled: *Integrated System for the Digital Analysis of Endoscopic Imaging Macrobiopsy for the Support of the Diagnosis of Gynaecological Cancer (IPPOKRATIS),* December 2002 – December 2004.

References

[1] J.A. Fayez, M.F. Vogel, 'Comparision of different treatment methods of endometriomas by laparoscopy', *Obstet. Gynecol.*, Vol. 78, pp. 660-665, 1991.

[2] R. Wenzl, R. Lehner, U. Vry, N. Pateisky, P. Sevelda, P. Husslein, 'Three-dimensional video-endoscopy: clinical use in gynaecological laparoscopy', *Lancet*, Vol. 344, pp. 1621–1622, 1994.

[3] M. S. Neophytou, C. S. Pattichis, V. Tanos, E. C. Kyriacou., D. Koutsouris, '*Texture Characterization of Gynaecological Tissue in Endoscopy: Preliminary Findings*', *CD-ROM Proceedings of the 1st MEDINF International Conference on Medical Informatics & Engineering*, 12-15 October, Craiova, Romania, 4 pages, 2003.

[4] S. A. Karkanis, D. K. Iakovidis, D. E. Maroulis, A. Karras Dimitris, M. Tzivras, 'Computer-aided tumor detection in endoscopic video using color wavelet features', *IEEE Transactions on Information Technology in Biomedicine,* Vol. 7(3), pp. 141-152, 2003.

[5] P. M. Tjoa, M. S. Krishnan, 'Feature extraction for the analysis of colon status from the endoscopic images', *BioMedical Engineering OnLine,* Apr. 2003, http://www.biomedical-engineering-online.com/content/2/1/9.

[6] M. S. Neophytou, C. S. Pattichis, M. S. Pattichis, V. Tanos, E. Kyriacou, D. Koutsouris, 'Multiscale Texture Feature Variability Analysis in Endoscopy Imaging Under Different Viewing Positions', *CD-ROM Proceedings of the II EFOMP Mediterranean Conference on Medical Physics*, 28-30 April, Limassol, Cyprus, 6 pages, 2004.

[7] R. M. Haralick, K. Shanmugam, I. Dinstein, 'Texture Features for Image Classification', *IEEE Trans. on Systems, Man., and Cybernetics,* Vol. SMC-3, pp. 610-621, Nov. 1973.

[8] P. P. Vaidyanathan, 'Multirate Systems and filter banks', *New Jersey: PTR Prentice Hall*, 1993.

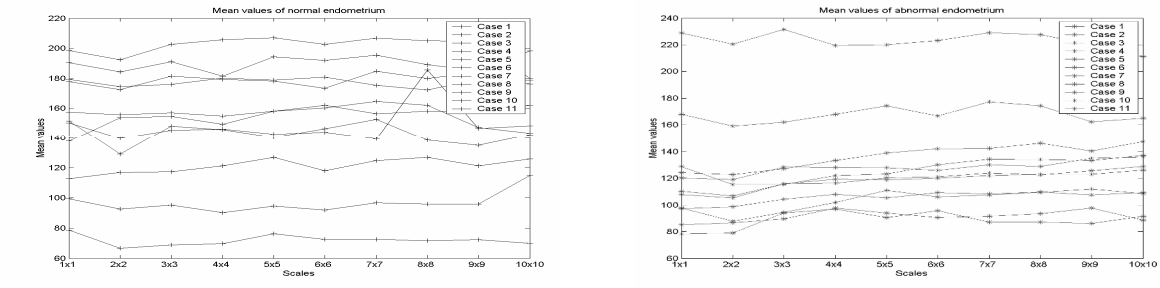

Fig. 5. Multiscale analysis for SF mean for normal (left) and abnormal (right) endometrium

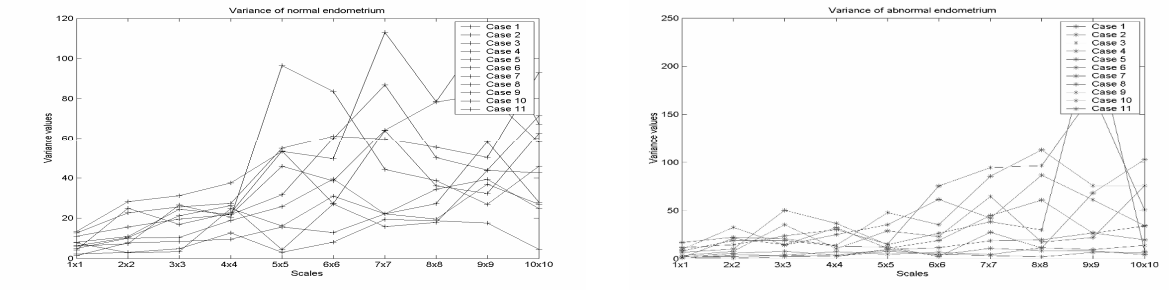

Fig. 6. Multiscale analysis for SF variance for normal (left) and abnormal (right) endometrium

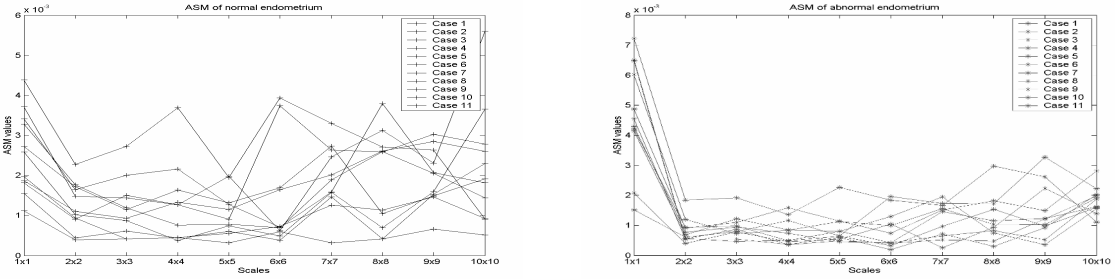

Fig. 7. Multiscale analysis for SGLDM ASM for normal (left) and abnormal (right) endometrium

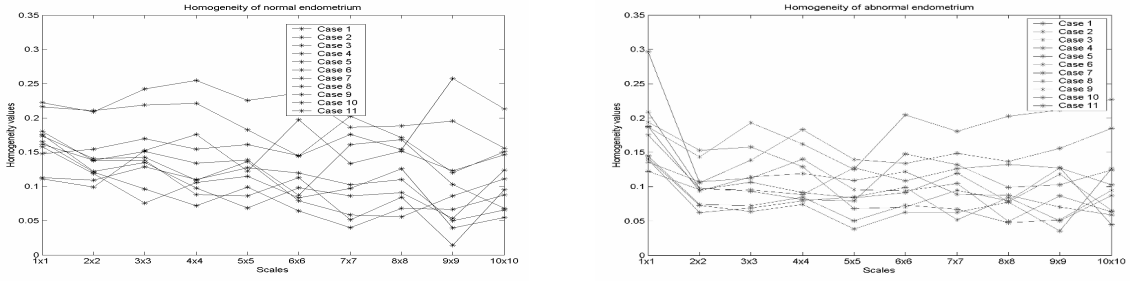

Fig. 8. Multiscale analysis for SGLDM homogeneity for normal (left) and abnormal (right) endometrium